The nuclear scaffold protein SAF-A is required for kinetochore–microtubule attachment and contributes to the targeting of Aurora-A to mitotic spindles

Nan Ma[1,*], Sachihiro Matsunaga[1,*,‡], Akihiro Morimoto[1,*], Gyosuke Sakashita[2], Takeshi Urano[2], Susumu Uchiyama[1] and Kiichi Fukui[1,‡]

[1]Department of Biotechnology, Graduate School of Engineering, Osaka University, Suita 565-0871, Japan
[2]Department of Biochemistry, Shimane University School of Medicine, Izumo 693-8501, Japan

*These authors contributed equally to this work
‡Authors for correspondence (sachi@bio.eng.osaka-u.ac.jp; kfukui@bio.eng.osaka-u.ac.jp)

Accepted 29 September 2010
Journal of Cell Science 124, 394-404

doi:10.1242/jcs.063347

Summary

Segregation of chromosomes during cell division requires correct formation of mitotic spindles. Here, we show that a scaffold attachment factor A (SAF-A), also known as heterogeneous nuclear ribonucleoprotein-U, contributes to the attachment of spindle microtubules (MTs) to kinetochores and spindle organization. During mitosis, SAF-A was localized at the spindles, spindle midzone and cytoplasmic bridge. Depletion of SAF-A by RNA interference induced mitotic delay and defects in chromosome alignment and spindle assembly. We found that SAF-A specifically co-immunoprecipitated with the chromosome peripheral protein nucleolin and the spindle regulators Aurora-A and TPX2, indicating that SAF-A is associated with nucleolin and the Aurora-A–TPX2 complex. SAF-A was colocalized with TPX2 and Aurora-A in spindle poles and MTs. Elimination of TPX2 or Aurora-A from cells abolished the association of SAF-A with the mitotic spindle. Interestingly, SAF-A can bind to MTs and contributes to the targeting of Aurora-A to mitotic spindle MTs. Our finding indicates that SAF-A is a novel spindle regulator that plays an essential role in kinetochore–MT attachment and mitotic spindle organization.

Key words: Aurora-A, Kinetochore–microtubule attachment, Mitosis, Nucleolin, SAF-A, Spindle assembly, TPX2

Introduction

Accurate chromosome segregation during cell division is essential for the integrity of the genome from generation to generation. Essential to this progress are the capture of kinetochores by microtubules (MTs) and chromosome congression at the spindle equator (Biggins and Walczak, 2003). One proposed mechanism for kinetochore–MT attachment is 'search-and-capture', in which centrosomes nucleate MTs at random, and the chromosomes capture and selectively stabilize the MTs (Kirschner and Mitchison, 1986). However, the centrosome-based search-and-capture might be insufficient to capture all of the kinetochores observed in living cells (Wollman et al., 2005).

The eukaryotic nucleus is a membrane-enclosed compartment supported by a complex scaffold or matrix of non-histone proteins (Podgornaya et al., 2003). Some nuclear scaffold proteins leave the nucleus at the time of nuclear envelope breakdown and are targeted to various mitotic apparati (Nickerson et al., 1992; Compton et al., 1992), whereas others, such as lamins, are dispersed throughout the cytoplasm (Jost et al., 1986). Because of the absence of the probes to identify and trace these proteins, we know very little about the fate and function of nuclear scaffold proteins during mitosis.

The chromosome peripheral protein nucleolin contributes to kinetochore–MT attachment and mitotic spindle assembly (Ma et al., 2007). Here, we report that scaffold attachment factor A (SAF-A), also known as heterogeneous nuclear ribonucleoprotein-U (hnRNP-U) (Fackelmayer and Richter, 1994), interacts with nucleolin during mitosis. SAF-A was originally found to be an abundant component of the nuclear scaffold in HeLa cells (Roming et al., 1992), which could be a target in apoptotic nuclear breakdown (Gohring et al., 1997), and can be involved in Wilms' tumor (Spraggon et al., 2007). Although many functions of SAF-A have been identified, the previous studies have not revealed its localization or functions during mitosis.

We demonstrate that SAF-A is localized at the spindles, spindle midzone and cytoplasmic bridge during mitosis. Using the RNA interference (RNAi) technique, cells depleted of SAF-A show a strong mitotic delay with reduced tension between the kinetochores of non-aligned chromosomes and decreased stability of kinetochore MTs. Moreover, SAF-A is involved in mitotic spindle assembly. The MT binding protein TPX2 is an essential factor for Ran-GTP-dependent MT nucleation around chromatin in frog egg extracts (Gruss et al., 2001; Wittmann et al., 2000) and is required for mitotic spindle assembly in mammalian cells (Gruss et al., 2002). TPX2 also binds to and activates Aurora-A kinase and targets it to spindle MTs (Kufer et al., 2002; Bayliss et al., 2003; Glover, 2003). Although the function of Aurora-A kinase is essential for multiple steps during mitosis (Barr and Gergely, 2007), only a few associated proteins have been identified. Here, we show that SAF-A is associated with both Aurora-A and TPX2. Interaction with the TPX2–Aurora-A complex is required for SAF-A binding to spindles. SAF-A also contributes to the targeting of Aurora-A to mitotic spindle MTs.

Journal of Cell Science

Results

Localization of SAF-A during mitosis

To identify proteins associated with nucleolin during mitosis, we used immunoprecipitation from mitotic HeLa cell extracts with an anti-nucleolin antibody. Fibrillarin, B23, and SAF-A were identified in the nucleolin co-immunoprecipitates using non-synchronized human kidney 293EBNA cells (Yanagida et al., 2001). These three proteins also interacted with nucleolin during mitosis (Fig. 1A). Consistently, the specific interaction between SAF-A and nucleolin during mitosis was confirmed by a GST pulldown assay (Li et al., 2009). We examined the expression level of SAF-A through the cell cycle using synchronized HeLa cells with arrest at the G1–S boundary by a double thymidine block, and at mitosis by adding nocodazole. Western blot analysis using whole cell lysates at S, G2, M and G1 phases showed that the cellular level of SAF-A was constant throughout the cell cycle (Fig. 1B). To examine the localization of SAF-A during mitosis, we performed immunostaining with an antibody against SAF-A (ab-10297) (Dreyfuss et al., 1984) on HeLa cells (Fig. 1C). At interphase, SAF-A was mainly localized in the nucleus. When the cells progressed to mitosis, SAF-A started to localize along spindle MTs (Fig. 1C). At metaphase, the SAF-A signals overlapped with the mitotic spindle (Fig. 1C,D). To determine whether SAF-A constitutes a genuine spindle component, we transiently expressed the EGFP-tagged protein in HeLa cells and analyzed its localization. Staining with α-tubulin showed that the EGFP-tagged SAF-A protein was colocalized with spindle MTs in mitotic cells (Fig. 1E). The detailed localization of SAF-A in the kinetochore was clarified by staining with an outer kinetochore marker protein CENP-F. Interestingly, the signals for SAF-A overlapped at the MT attachment side with those for CENP-F, suggesting that SAF-A is localized adjacent to the outer kinetochore (Fig. 1F). SAF-A

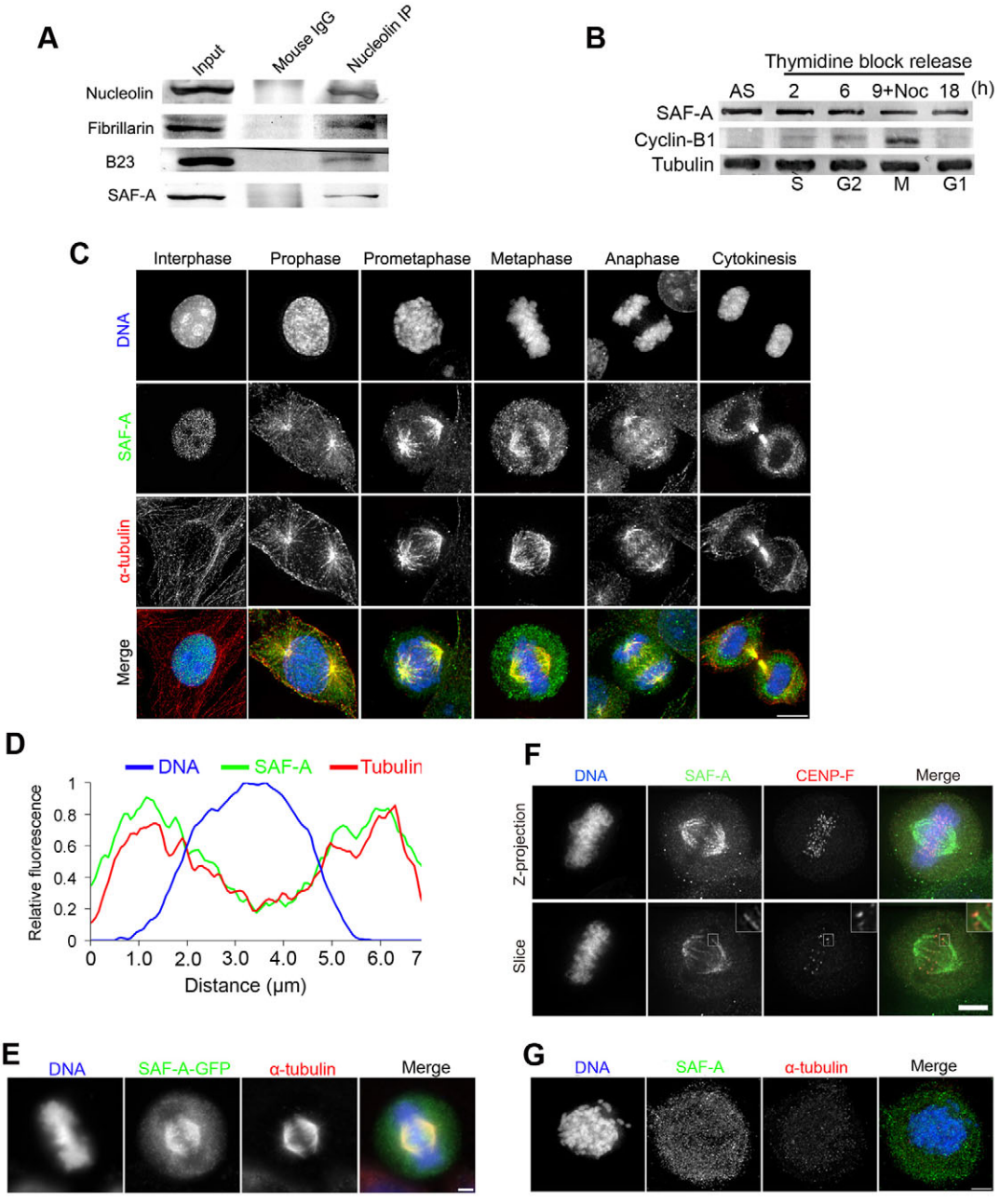

Fig. 1. Dynamic localization of SAF-A during mitosis. (**A**) Immunoblot analysis of complexes pulled down from mitotic cell extracts by an anti-nucleolin antibody. Protein G beads coupled to mouse IgG were used as controls. (**B**) Immunoblot analysis using HeLa cells synchronized with thymidine and nocodazole (Noc). After release, the cell lysates were immunoblotted with antibodies against SAF-A, α-tubulin and the M-phase marker cyclin B1. Asynchronous (AS) cell lysates were used as a loading control. (**C**) HeLa cells were stained for SAF-A (green) and α-tubulin (red) at different phases of the cell cycle. (**D**) Averaged fluorescence intensity was derived from ten line scans of the relative fluorescence intensity from a pole to an opposite pole. The line scan was performed in the sum projection of the metaphase cell. (**E**) Cells transiently expressing SAF-A–EGFP were stained for α-tubulin (red). (**F**) Mitotic HeLa cells were stained for SAF-A (green) and CENP-F (red). The lower panel shows an optical section. The enlarged inset shows a kinetochore region. (**G**) Cells were treated with colcemid and stained for SAF-A (green) and α-tubulin (red). Scale bars: 5 μm.

signals were also detected in the spindle midzone at anaphase and were eventually concentrated in the cytoplasmic bridge at telophase (Fig. 1C). Immunostaining with another anti-SAF-A antibody (sc-32315) (Kukalev et al., 2005) produced the same localization pattern of SAF-A during mitosis (data not shown). When MTs were depolymerized with colcemid, the SAF-A signals were dispersed into the cytoplasm (Fig. 1G), supporting that localization of SAF-A in mitotic spindles is dependent on MTs.

Effect of SAF-A depletion on mitotic spindle assembly

To explore the function of SAF-A, we depleted SAF-A with two different siRNA sequences (SAF-A-specific siRNA1 and siRNA2). Both siRNA sequences efficiently and specifically reduced the expression level of SAF-A (Fig. 2A; supplementary material Fig. S1) so we used siRNA1 in further studies. Two types of abnormal spindles, unstable and disorganized spindles, were found in SAF-A-depleted cells. Unstable spindles showed an absence of, or irregular, spindle poles. Disorganized spindles exhibited a large reduction in the number of MT connections between the two asters and chromosomes, although the asters had many MTs (Fig. 2B). SAF-A-depleted cells showed an approximately five- to sevenfold increase in spindle defects when cells were examined at 72 hours after RNAi transfection with siRNA1 or siRNA2 (Fig. 2C). Consistently, when the cells were transfected with siRNA immediately after plating, 15.0% of the SAF-A-depleted cells showed spindle defects at 48 hours after siRNA transfection. Spindle defects were greater than 3.5% in control cells (supplementary material Fig. S2A,B), demonstrating that the phenotype in SAF-A depletion was not derived from the accumulation of multiple defects in interphase. Similar to that of nucleolin-depleted cells, the mitotic index of the SAF-A-depleted cells was 6.4±1.0%, which was greater than that of control cells (2.7±0.3%) (supplementary material Fig. S3A). Double knockdown of both SAF-A and nucleolin did not further increase the mitotic index compared with SAF-A-depleted cells (supplementary material Fig. S3A), suggesting that SAF-A and nucleolin interact co-operatively to regulate mitotic events. Consistent with the increased mitotic index, the population of cells at G2–M phase detected by flow cytometry was increased in the absence of SAF-A, compared with control cells (Fig. 2D). Among SAF-A-depleted cells, 66.2±8.8% of the mitotic cells were in prometaphase, whereas 19.7±3.0% of mitotic cells in control cells were in prometaphase (supplementary material Fig. S3B).

Effect of SAF-A depletion on chromosome alignment

Next, we compared the chromosome alignment in control cells to that in SAF-A depleted cells. In control cells, the kinetochores were distributed within the mitotic spindle during prometaphase (Fig. 2E). However, in SAF-A depleted cells, some kinetochores were frequently localized outside the spindle (Fig. 2E; supplementary material Fig. S4A). SAF-A depletion induced two types of defect in chromosome congression: misalignment and non-alignment (Fig. 2E). In the misalignment phenotype, less than ten chromosomes remained outside the spindle, although the other chromosomes aligned at the spindle equator. In the non-alignment phenotype, more than ten chromosomes were dispersed outside the spindle. In mitotic cells depleted by siRNA1, the misalignment and non-alignment phenotypes were found in 12.1% and 15.1% of cells, respectively (Fig. 2F). By contrast, the control cells rarely showed either phenotype (2.4% and 1.0%, respectively). Inhibition of proteosome activity with MG132 did not decrease the frequencies of either phenotype in SAF-A-depleted cells (data not shown). These findings indicate that the defects in chromosome congression are actually generated before the onset of anaphase. Similar to the results of 72-hour depletion, a significant increase in defects in chromosome congression was observed when cells were examined after 48-hour depletion (supplementary material Fig. S2C; 13.1% in SAF-A-depleted cells versus 5.1% in control cells).

We tested the possibility that the defects in chromosome congression in SAF-A-depleted cells might be due to an abnormality in MT attachment to the kinetochore. In control cells, bi-oriented kinetochores were frequently observed with robust kinetochore MTs terminating at the kinetochores (supplementary material Fig. S4A). In the misalignment phenotype, chromosomes near the spindle poles frequently attached to MTs monotelically (supplementary material Fig. S4A, enlargement a) or syntelically (supplementary material Fig. S4A, enlargement b). In the non-alignment phenotype, some chromosomes were unable to attach to MTs (supplementary material Fig. S4A).

Effect of SAF-A depletion on MT and chromosome dynamics

Next, to further confirm the defects in fixed samples, we used time-lapse microscopy to analyze mitosis using live cells stably expressing fluorescent protein-tagged proteins. We performed SAF-A RNAi in cells expressing yellow fluorescent protein (YFP)-tagged α-tubulin, and imaged spindle MT mobility at highly temporal resolution (Fig. 3A). The majority of control cells formed the bipolar spindle and completed cytokinesis within 35 minutes. By contrast, 9.3% and 23.1% of the mitotic spindles in SAF-A-depleted cells exhibited unstable and disorganized spindles, respectively (Fig. 3B). By contrast, the control cells rarely showed either phenotype (1.5% and 4.8%, respectively). We also analyzed chromosome dynamics using live cells stably expressing green fluorescent protein (GFP)-tagged histone H1.2 (GFP-H1.2) (Gambe et al., 2007). Non-aligned chromosomes and mitotic delay were frequently observed in SAF-A-depleted cells (Fig. 3C,D). Surprisingly, despite the prolonged prometaphase, 56.7% of the SAF-A-depleted cells containing non-aligned chromosomes initiated anaphase without complete chromosome congression (Fig. 3C,E). We also demonstrated that the chromosome congression defects in SAF-A-depleted cells were not due to the loss of Aurora-B (supplementary material Fig. S5A), Hec1 (supplementary material Fig. S5B) or CENP-E (data not shown) at kinetochores, or the loss of nucleolin in the vicinity of kinetochores (data not shown), because their localization was unchanged after SAF-A depletion. Moreover, we showed that the mitotic delay occurring in SAF-A-depleted cells resulted from activation of the spindle checkpoint because we detected spindle checkpoint proteins including Bub1, BubR1 and Mad2 at the kinetochores of non-aligned chromosomes in SAF-A-depleted cells (supplementary material Fig. S3C). Consistently, inactivation of the spindle checkpoint by RNAi for Mad2 rescued the mitotic delay in SAF-A-depleted cells (supplementary material Fig. S3D).

Effect of SAF-A depletion on MT nucleation activity

To examine the MT nucleation activity at centrosomes, cells were placed on ice for 30 minutes to disrupt cellular MT organization, and then transferred to 37°C to initiate MT organization. Twenty seconds later, the cells were fixed and immunostained. We detected similar MT asters at centrosomes in both control and SAF-A-depleted cells (Fig. 4A). Next, we examined the MT nucleation

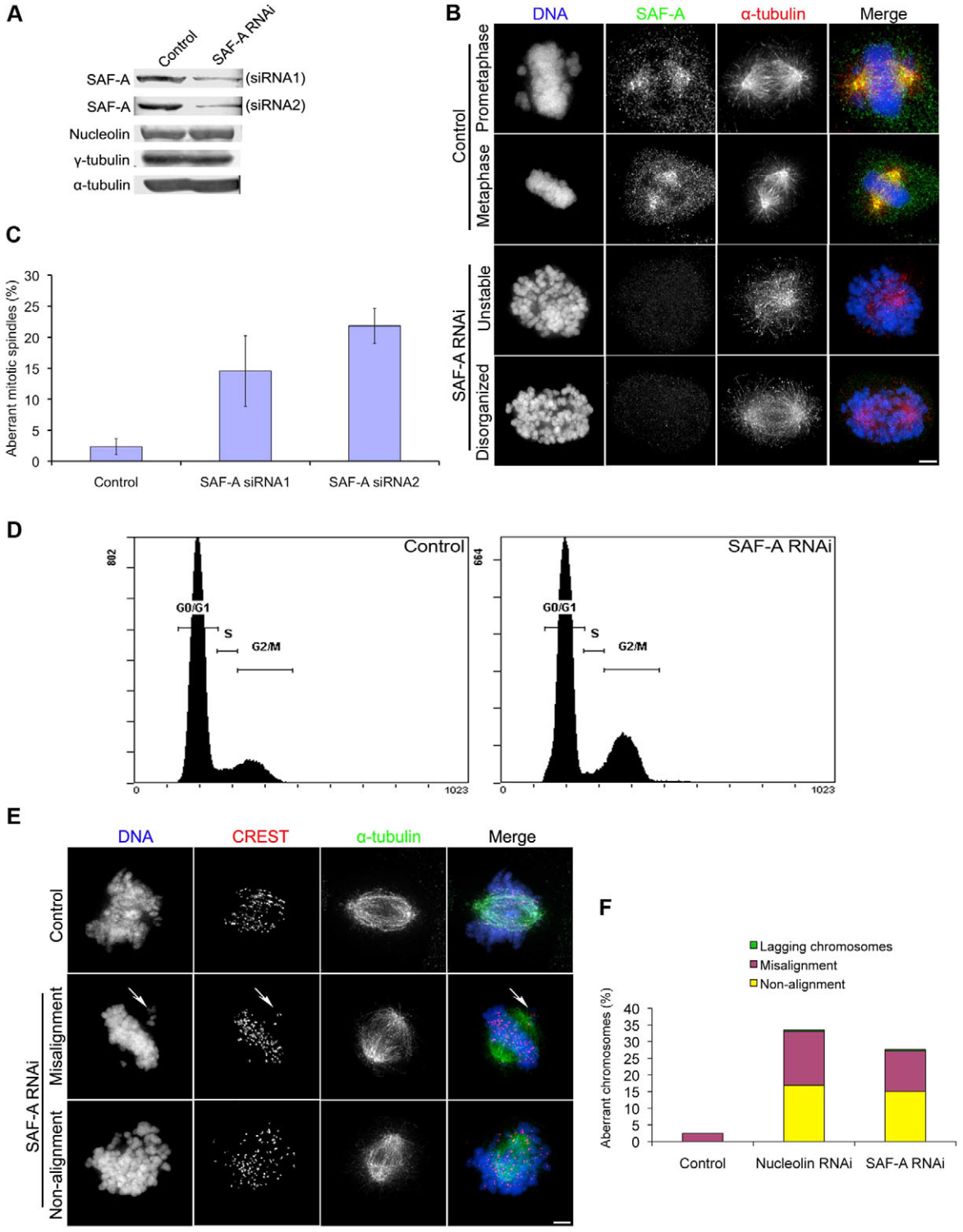

Fig. 2. SAF-A depletion induces defects in mitotic spindle assembly and chromosome congression. (**A**) Immunoblot showing effective depletion of SAF-A by two siRNAs. The expression levels of nucleolin, α-tubulin and γ-tubulin were not changed. (**B**) Mitotic spindle defects in SAF-A-depleted cells. The unstable and disorganized spindle phenotypes are shown. Cells were stained for SAF-A (green) and α-tubulin (red). (**C**) Quantification of mitotic spindle defects after SAF-A depletion with two siRNAs. Values are means±s.d. of four independent experiments (n=400). (**D**) SAF-A depletion increased the G2–M cell populations. Propidium iodide-stained HeLa cells were analyzed by flow cytometry after siRNA transfection. The cell populations at the G0–G1, S and G2–M phases were divided based on the relative fluorescence intensity; 5.0×10^4 cells were counted in each condition. (**E**) The prometaphase phenotype of a control cell and misalignment and non-alignment phenotypes of SAF-A-depleted cells. Cells were stained with anti-α-tubulin (green) antibody and CREST (red). Arrows show misaligned chromosomes. (**F**) Quantification of the distribution of chromosome congression defects after transfection with siRNAs targeting nucleolin and SAF-A. Values are means of four independent experiments (n=400).

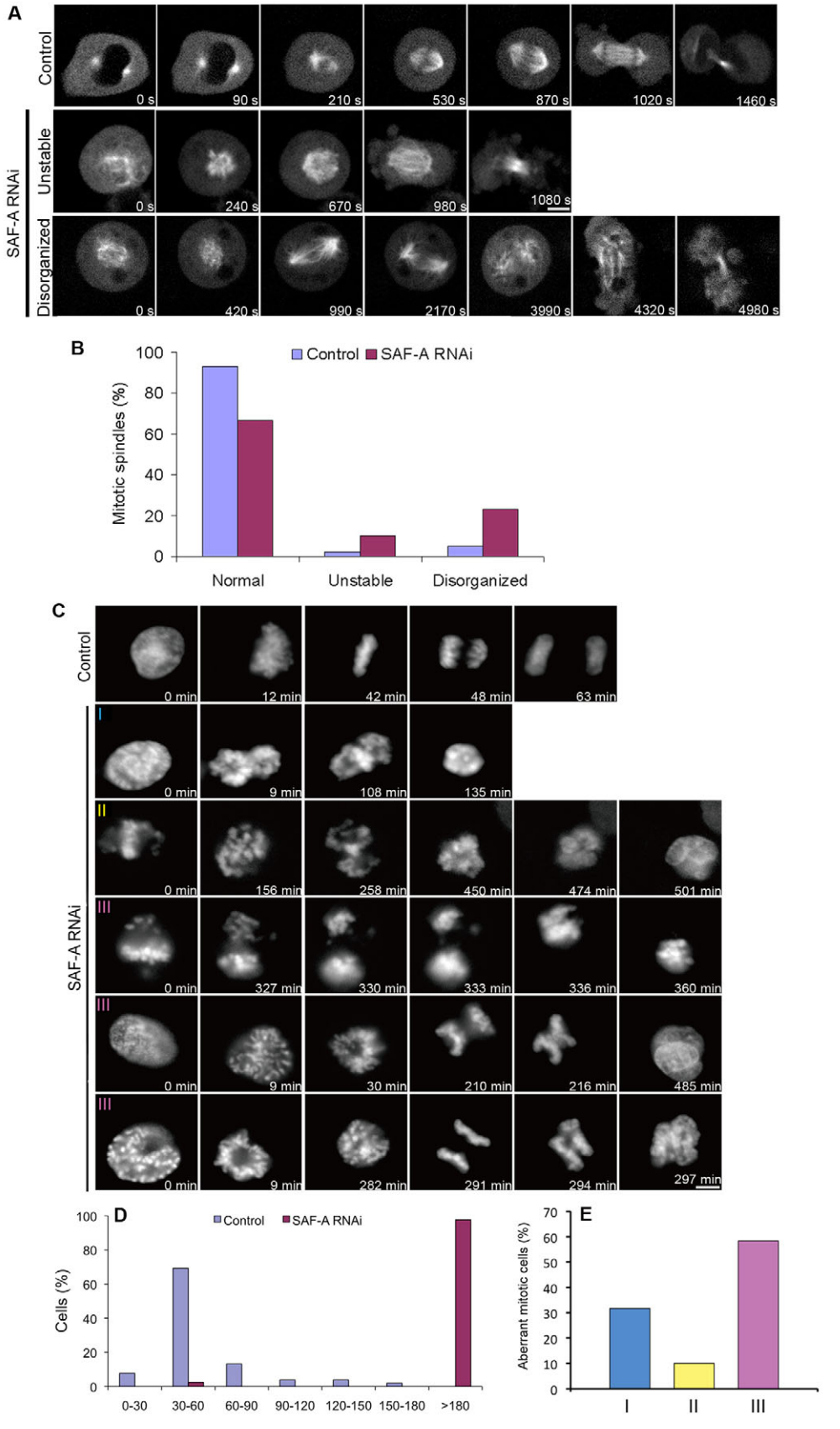

Fig. 3. SAF-A depletion induces defects in the dynamics of MTs and chromosomes. (**A**) Microtubule dynamics analyzed by live cell imaging. HeLa cells stably expressing YFP–α-tubulin were imaged by time-lapse fluorescence microscopy after siRNA transfection. SAF-A-depleted cells showed unstable or disorganized spindles. Times are given in seconds. (**B**) Frequencies of defects in spindle assembly in the control (n=25) and SAF-A-depleted (n=22) cells shown in A. (**C**) Chromosome dynamics analyzed by live cell imaging. HeLa cells stably expressing GFP–H1.2 were imaged by time-lapse fluorescence microscopy after siRNA transfection. Times are given in minutes. In SAF-A-depleted cells, three types of aberrant chromosome behaviors (I–III) were observed. I: Chromosomes never align on the spindle equator after a long period of arrest at the prometaphase. II: Chromosomes never align on the spindle equator after a long period of arrest at prometaphase; the chromosomes then decondense into micronuclei. III: Chromosomes never align on the spindle equator after a long period of arrest at the prometaphase, and anaphase is initiated in the presence of non-aligned chromosomes, but chromosomes are not able to separate successfully in cytokinesis. (**D**) Percentages of cells with different durations of mitosis. Control (n=53) and SAF-A-depleted cells (n=60) were analyzed by time-lapse fluorescence microscopy. (**E**) Frequencies of aberrations of chromosome dynamics in SAF-A-depleted cells. Categories I–III correspond to the numbers indicated in C. Scale bars: 10 μm.

activity near the kinetochores. Cells were treated with 3.3 µM nocodazole for 3 hours to completely disassemble MTs, washed twice with drug-free media, and then incubated at 37°C. After 10 minutes, the cells were fixed and immunostained. In control and SAF-A-depleted cells, MTs formed at discrete sites on kinetochores (Fig. 4B). Consistent with the report that TPX2 is required for kinetochore-associated MT formation (Tulu et al., 2006), MTs did not re-grow at kinetochores in TPX2-depleted cells (Fig. 4B). Taken together, these data suggest that SAF-A depletion does not influence the nucleation activity of MTs at centrosomes or kinetochores.

To determine whether SAF-A-depleted cells can establish stable kinetochore–MT attachment, we performed a cold-mediated depolymerization assay. When cells are subjected to cold treatment for a short period time, the less-stable MTs are depolymerized first, preferentially leaving stabilized MT populations such as kinetochore–MTs intact (Rieder, 1981). When the stability of kinetochore–MTs is compromised, they also depolymerize in this assay (Ma et al., 2007). In the control prometaphase cells, not all of the chromosomes became bi-oriented and some chromosomes were unable to align at the spindle equator (Fig. 4C). In the control

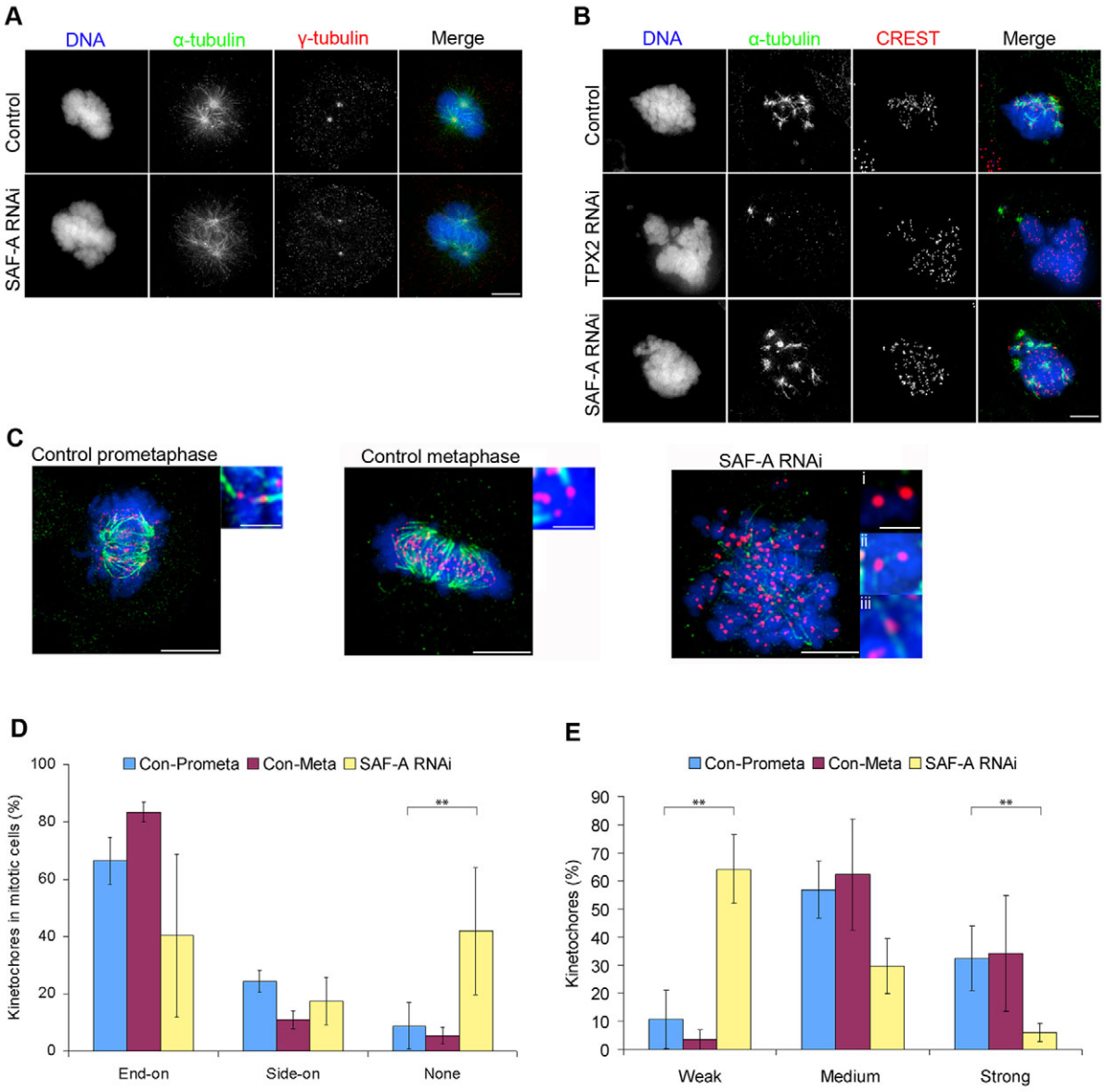

Fig. 4. SAF-A is not required for MT nucleation but is required for stable kinetochore–MT attachment. (**A**) The MT re-growth assay at centrosomes was performed with control and SAF-A-depleted cells. The cells were immunostained with antibodies against α-tubulin (green) and γ-tubulin (red). (**B**) The MT re-growth assay at kinetochores was performed with control, SAF-A- and TPX2-depleted cells. The cells were immunostained with antibodies against α-tubulin (green) and CREST (red). (**C**) Control or SAF-A-depleted cells were exposed to cold and stained with anti-α-tubulin antibody (green) and CREST (red). The insets are enlarged fourfold. Insets i, ii and iii indicate an absence of, end-on and side-on MT attachment, respectively. (**D**) Proportions of kinetochores with end-on, side-on or no MT attachment in control prometaphase cells (n=6), control metaphase cells (n=10) and SAF-A-depleted cells (n=11). Optical sections were taken through the thickness of the cell, and at least ten kinetochores were evaluated in each cell for their attachment to MTs. (**E**) Quantification of stable kinetochore–MTs in cells exposed to cold. Bar graphs indicate the percentage of kinetochores lacking attached MTs, having a weak attachment, a medium attachment, or a strong attachment in control (n=194) and SAF-A-depleted (n=186) cells. All values are means±s.d. **P<0.01. Scale bars: 5 µm; 1.25 µm in enlargements.

metaphase cells, the MTs remained intact and demonstrated bipolar attachment to kinetochore pairs (Fig. 4C). By contrast, the majority of SAF-A-depleted cells exhibited a disappearance of kinetochore–MTs and reduced attachment between kinetochores and spindle MTs after cold treatment (Fig. 4C), suggesting that kinetochore–MTs were not stable when SAF-A was depleted. Following the cold-mediated depolymerization assay, examination of optical sections of SAF-A-depleted cells revealed that 42.0±22.2% of kinetochores had no attachment to spindle MTs (Fig. 4D). By contrast, only 8.9±8.1% of control prometaphase and 5.5±2.8% of control metaphase cells showed no kinetochore–MT attachment. There was little change between control and SAF-A-depleted cells in the number of kinetochores with slide-on attachments (Fig. 4D). Furthermore, we quantified kinetochore–MT intensity in the vicinity of kinetochores as previously described (Toso et al., 2009). Depletion of SAF-A abolished the number of stable kinetochore–MTs in bipolar spindles as compared with the control cells (64.2±12.3% kinetochores with a weak signal vs 10.7±10.4% for control cells; Fig. 4E). We conclude that SAF-A depletion reduces the number of stable kinetochore–MTs. In addition, using CENP-A as a marker to measure the inter-kinetochore distance, which reflects tension across kinetochore pairs (Waters et al., 1996), we found that the non-aligned chromosomes in SAF-A-depleted cells showed a significant decrease in inter-kinetochore distance compared with the control cells (supplementary material Fig. S4B,C). Taken together, these data indicate that SAF-A is required for kinetochore–MT attachment and to stabilize kinetochore MTs, which are essential for chromosome congression.

SAF-A interaction with Aurora-A and TPX-2

To search for proteins that interact with SAF-A, several antibodies were used to immunoprecipitate SAF-A from mitotic cell extracts. We detected the association of SAF-A with TPX2 and vice versa (Fig. 5A,B). Interestingly, SAF-A was also immunoprecipitated with an anti-Aurora-A antibody (Fig. 5C). These results suggest that SAF-A is associated with the Aurora-A–TPX2 complex. SAF-A localization was overlapped with the TPX2 localization in spindle poles and MTs (Fig. 5D) and with Aurora-A localization in spindle poles and spindle MTs proximal to spindle poles (Fig. 5E). To explore the functional significance of the interactions among SAF-A, Aurora-A and TPX2, these three proteins were silenced by RNAi. SAF-A depletion induced significant reduction of Aurora-A in the spindle MTs (Fig. 5E,G; supplementary material Fig. S6B) whereas SAF-A depletion did not significantly affect the localization of TPX2 (Fig. 5D,F; supplementary material Fig. S6A). Thus, an essential function of SAF-A is to recruit Aurora-A to the mitotic spindle MTs. In the absence of TPX2 or Aurora-A, SAF-A was largely disassociated from spindle MTs (Fig. 5D,E,H; supplementary material Fig. S6C), indicating that the binding of SAF-A to spindle MTs is dependent on Aurora-A and TPX2. Because Aurora-A was associated with SAF-A (Fig. 5A), we investigated whether Aurora-A phosphorylates SAF-A in vitro. We performed the phosphorylation assay in the presence of [γ-^{32}P]ATP using isolated SAF-A from HeLa cells (supplementary material Fig. S7). The autophosphorylation of Aurora A and the phosphorylation of histone H3(5-15) were detected as described previously (Ohashi et al., 2006). However, we did not detect significant phosphorylation of SAF-A in vitro by Aurora-A. Finally, to determine whether SAF-A binds to MTs directly, isolated SAF-A or recombinant TPX2 protein was incubated with taxol-stabilized MTs in a co-pelleting assay. The results showed that isolated SAF-A protein co-pelleted with stabilized MTs in a TPX2-dependent manner (Fig. 6).

Discussion

Here, we describe the localization and functional analysis of human SAF-A during mitosis. Knockdown of SAF-A caused multiple events to fail in mitosis, causing mitotic delay, abnormal alignment of chromosomes and defects in spindle assembly. Strikingly, SAF-A interacts with both TPX2 and Aurora-A, and contributes to the localization of Aurora-A on spindle MTs. Although we cannot exclude the possibility that knockdown of SAF-A interferes with interphase events, the evidence supports the idea that SAF-A is an essential component of the mitotic spindle. First, SAF-A was one of the proteins identified in the proteome analysis of human mitotic spindle (Sauer et al., 2005; Nousiainen et al., 2006). Second, immunostaining for SAF-A and the expression of SAF-A–EGFP clearly demonstrated the SAF-A localization at mitotic spindles. Third, SAF-A depletion did not significantly influence the expression level of many mitotic proteins (e.g. Hec1, Aurora A, Aurora B and TPX2). This result excludes the possibility that the aberrant spindles in SAF-A-depleted cells resulted from depletion of these mitotic proteins, and supports the idea that these aberrations reflect the effect of SAF-A depletion (supplementary material Fig. S1B). Finally, SAF-A has recently been identified as one of the proteins required for chromosome segregation in genome-wide RNAi screening (Hutchins et al., 2010). Taken together, the results lead us to believe that the mitotic defects following SAF-A depletion by RNAi reveal the functions of SAF-A during mitosis, and that these are not derived from the secondary effects caused by the defects in gene expression or regulation during interphase.

Functions of SAF-A in kinetochore–MT attachment and spindle assembly during mitosis

Nucleolin has been reported to localize to the chromosome periphery during mitosis (Ma et al., 2007). Depletion of nucleolin led to a prolonged cell cycle and to chromosome misalignment. In addition, the results of cold treatment experiments indicated that kinetochore–MTs become unstable in the absence of nucleolin. Because nucleolin does not bind directly to MTs (Li et al., 2009), the detailed mechanism of nucleolin in the stabilization of kinetochore–MTs remains unclear.

The failure of the stable bipolar attachment phenotype indicates that SAF-A functions in one or more steps in the kinetochore–MT interaction, including initial capture and MT stabilization or formation of mature attachments. Interestingly, protein PinX1, which is localized at the outer kinetochore and chromosome periphery, is associated with both nucleolin and SAF-A (Li et al., 2009) and is required for chromosome segregation during mitosis (Yuan et al., 2009). Our results are consistent with a model in which MT-associated SAF-A binds to the outer kinetochore through interaction with PinX1 and nucleolin to stabilize kinetochore–MT attachments. SAF-A is associated with nucleolin and PinX1 at the outer kinetochore, and is associated with Aurora-A and TPX2 at spindle MTs, suggesting that SAF-A plays multiple roles during mitosis, in different intracellular regions and in different complexes. Moreover, because the majority of the cells without proper localization of Aurora-A at spindle MTs are able to align their chromosomes normally at the spindle equator and complete chromosome segregation (Bird and Hyman, 2008), the mitotic

defects observed in SAF-A-depleted cells could be mainly due to the loss of SAF-A function rather than to loss of localization of Aurora-A at mitotic spindles.

SAF-A is associated with the Aurora-A–TPX2 complex and contributes to the targeting of Aurora-A to spindle MTs

In this study, we also demonstrated that SAF-A interacts with both Aurora-A and TPX2 during mitosis. The TPX2–SAF-A interaction is required to recruit SAF-A to spindle MTs in vivo and to form SAF-A–tubulin co-pellets in vitro. Similarly, TPX2 is also required to target proteins including Xklp2 (*Xenopus* kinesin-like protein 2), Aurora-A and Kif15 to spindles during mitosis (Wittmann et al., 2000; Kufer et al., 2002; Tanenbaum et al., 2009). Thus, TPX2 could form an adapter for loading various proteins onto the mitotic spindle (Garrett et al., 2002). In turn, this might help bring SAF-A onto the spindle MTs (including the plus ends of MTs) to help the formation of the correct kinetochore–MT attachment and bring Aurora-A into close proximity to its potential substrates. Furthermore, it is clear that Aurora-A is required for targeting SAF-A onto spindle MTs. Thus, Aurora-A could help to maintain

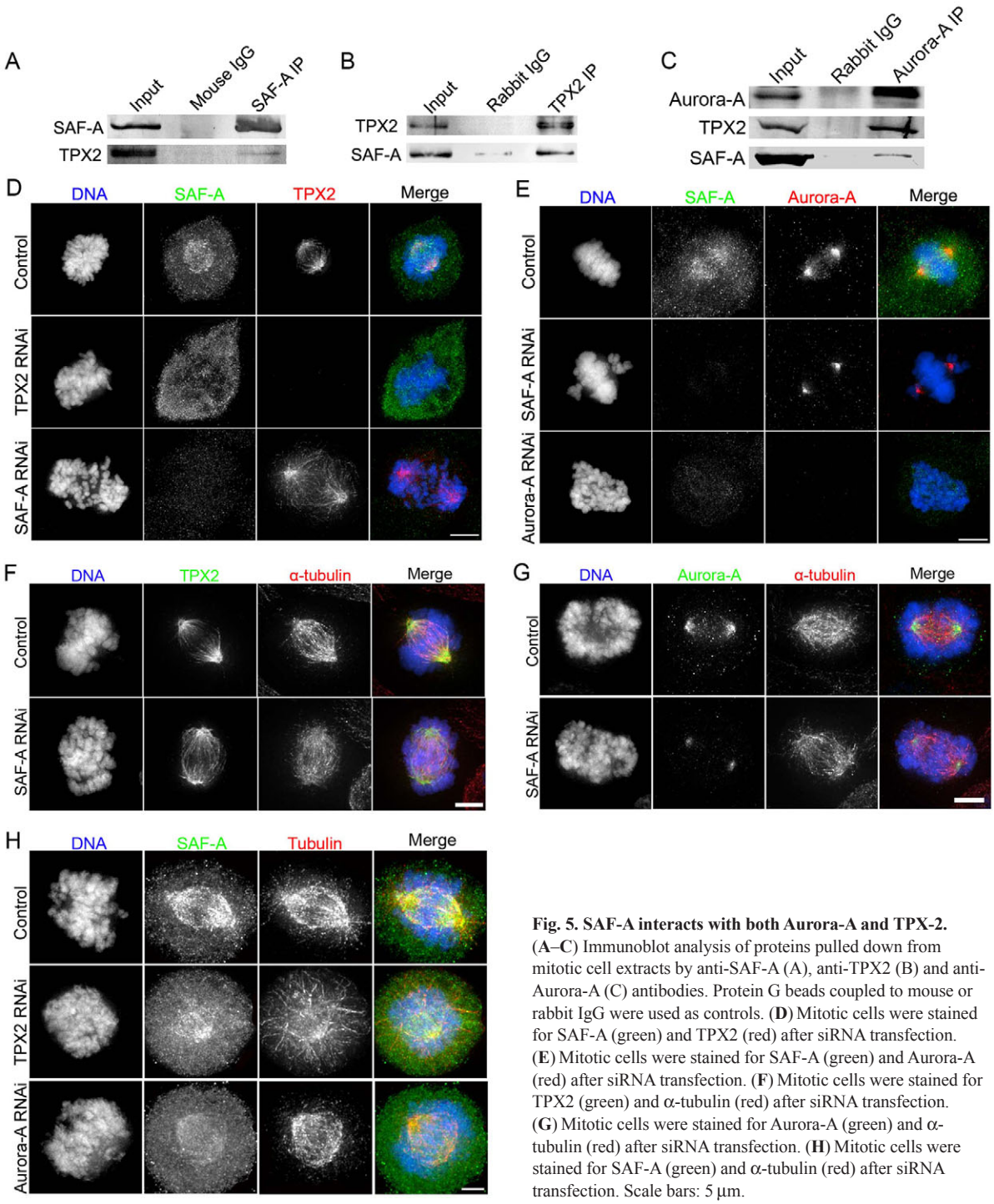

Fig. 5. SAF-A interacts with both Aurora-A and TPX-2. (**A**–**C**) Immunoblot analysis of proteins pulled down from mitotic cell extracts by anti-SAF-A (A), anti-TPX2 (B) and anti-Aurora-A (C) antibodies. Protein G beads coupled to mouse or rabbit IgG were used as controls. (**D**) Mitotic cells were stained for SAF-A (green) and TPX2 (red) after siRNA transfection. (**E**) Mitotic cells were stained for SAF-A (green) and Aurora-A (red) after siRNA transfection. (**F**) Mitotic cells were stained for TPX2 (green) and α-tubulin (red) after siRNA transfection. (**G**) Mitotic cells were stained for Aurora-A (green) and α-tubulin (red) after siRNA transfection. (**H**) Mitotic cells were stained for SAF-A (green) and α-tubulin (red) after siRNA transfection. Scale bars: 5 µm.

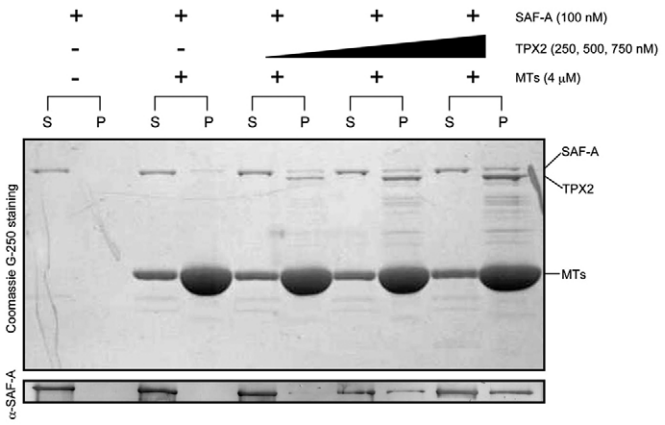

Fig. 6. SAF-A binds to MT in a TPX2-dependent manner. MT binding analysis of isolated SAF-A protein in the presence of different amounts of recombinant TPX2 protein. The lower panel shows western blotting with anti-SAF-A antibody. SAF-A co-pelleted with MT was increased, dependent on the amount of TPX2. S, supernatant; P, pellet.

SAF-A on the spindle MTs directly or indirectly by phosphorylation of SAF-A-interacting proteins.

MT nucleation near the kinetochores was normal in SAF-A-depleted cells, although most of the Aurora-A lost its localization on spindle MTs. In fact, very little is known about Aurora-A-mediated MT nucleation near kinetochores in vivo, in contrast to TPX2-mediated MT nucleation at kinetochores. FRAP analysis has shown that Aurora-A moves very rapidly ($t_{1/2}$ of ~3 seconds) between the mitotic spindle and cytoplasm of the mitotic spindle in a MT-independent manner (Stenoien et al., 2003), indicating a continuous exchange of Aurora-A on the spindle MTs (Blagden and Glover, 2003; Barr and Gergely, 2007). Even when Aurora-A does not localize on the spindle MTs, Aurora-A activated by TPX2 can promote MT nucleation in vitro (Sardon et al., 2008). Therefore, we cannot exclude the possibility that Aurora-A at spindle poles, or rapidly exchanged cytoplasmic Aurora-A on spindle MTs after SAF-A RNAi, supplies phosphorylated substrates to assist MT nucleation near kinetochores. It is known that TPX2 can activate Aurora-A directly (Bayliss et al., 2003), but spindle MTs further enhance this activation (Kufer et al., 2003). In addition to a function in kinetochore–MT attachment, SAF-A has a plausible function in enhancing the activation of Aurora-A by targeting it onto spindle MTs.

We compared the functions of Aurora-A, TPX2 and SAF-A during mitosis (Table 1). All three proteins contribute to chromosome congression, kinetochore–MT attachment and stability of kinetochore MTs. Intriguingly, both Aurora-A and TPX2 accumulate at the spindle poles and function in the nucleation of MTs near the chromosomes (Katayama et al., 2008; Bird and Hyman, 2008), which differ from the localization and function of SAF-A during mitosis. Therefore, it is possible that SAF-A transiently interacts with the Aurora-A–TPX2 complex during mitosis.

In summary, SAF-A is a newly characterized and essential component of the mitotic apparatus. SAF-A acts in different multi-component complexes that affect the stability of kinetochore–MT attachments, and contributes to the targeting of Aurora-A to spindle MTs.

Table 1. Comparison of Aurora-A, TPX2 and SAF-A functions during mitosis

Mitotic event	Aurora-A	TPX2	SAF-A
G_2–M transition	+[1]	–*	–*
Centrosomal γ-tubulin recruitment	–[2]	–[3]	–*
Spindle biopolarity	+[4]	+[3]	–*
MT nucleation from centrosomes	+[5]	–[6]	–*
MT nucleation from chromosomes	+[7]	+[6]	–*
Chromosome congression	+[2,4]	+[3,8]	+*
Stability of kinetochore fibers	+[7]	+[7]	+*
Kinetochore–MT attachment	+[9]	+[10]	+*
Cytokinesis	+[2]	N/A	+*

+ and – indicate affected and not affected, respectively. *Data presented in this paper or unpublished data; [1]Hirota et al., 2003; [2]Marumoto et al., 2003; [3]Garrett et al., 2002; [4]Girdler et al., 2006; [5]Sardon et al., 2008; [6]Tulu et al., 2006; [7]Bird and Hyman, 2008; [8]Gruss et al., 2002; [9]Kunitoku et al., 2003; [10]Manning and Compton, 2007.

Materials and Methods

Cell synchronization by nocodazole treatment and double-thymidine block

HeLa cells were grown in DMEM (GIBCO BRL) supplemented with 10% fetal bovine serum (Hyclone) and penicillin. For S phase synchronization, cells were treated twice with 2.5 mM thymidine (Sigma) for 16 hours each, separated by a 10-hour exposure to culture medium. Mitotic arrest was induced by adding 100 ng/ml nocodazole to the culture medium and incubating the cells for 16 hours. Cell lysates were then prepared and immunoblotted.

Plasmid construction

The SAF-A (isoform b) clone in pET21-a was a kind gift from Paul R. Clarke (University of Dundee, Dundee, Scotland) (Berglund and Clarke, 2009). SAF-A was amplified by PCR and cloned into the pEGFP–C1 expression vector using the *Age*I and *Nhe*I restriction enzyme sites.

RNAi depletion of SAF-A, nucleolin, Aurora-A, TPX2 and Mad2 in HeLa cells

A nonspecific siRNA duplex (Qiagen) was used for control transfections. Two siRNA duplexes (siRNA1: 5′-GAACUCUCGUAUGCUAAGATT-3′ and siRNA2: 5′-CGUAUUGGCUGGUCACUAATT-3′), targeting human SAF-A, were used to deplete SAF-A. Previously reported siRNA duplexes were used to deplete nucleolin (Ma et al., 2007), Aurora-A (Kufer et al., 2002), TPX2 (Gruss et al., 2002) and Mad2 (Tang et al., 2004). HeLa cells were transfected with siRNA duplexes using Lipofectamine 2000 (Invitrogen), and then immunoblotted and immunostained 48 hours after the transfection with siRNAs targeting Aurora-A or TPX2, or 72 hours after the transfection with siRNAs targeting SAF-A, nucleolin or Mad2.

Antibodies

The following antibodies were used: SAF-A (mouse monoclonal antibody; Abcam, ab-10297), SAF-A (mouse monoclonal antibody; Santa Cruz Biotechnology, sc-32315), nucleolin (mouse monoclonal antibody; Santa Cruz Biotechnology), α-tubulin (mouse monoclonal antibody; Calbiochem), α-tubulin (rabbit polyclonal antibody; Abcam), γ-tubulin (rabbit monoclonal antibody; Sigma), BubR1 (mouse monoclonal antibody; BD Transduction Laboratories), Bub1 (mouse monoclonal antibody; Chemicon), CENP-E (mouse monoclonal antibody; Abcam), CENP-A (mouse monoclonal antibody; Abcam), Aurora-B (rabbit polyclonal antibody; Abcam), fibrillarin (rabbit polyclonal antibody; Abcam), CREST (human monoclonal antibody; Cortex Biochem), Mad2 (rabbit polyclonal antibody; Covance), B23 (goat polyclonal antibody; Santa Cruz Biotechnology), Cdc27 (mouse monoclonal antibody; Abcam), Cdc20 (mouse monoclonal antibody; MBL), Cyclin B1 (rabbit monoclonal antibody; Sigma), Aurora-A (rabbit polyclonal antibody; Bethyl Laboratories), hnRNP-G (goat polyclonal antibody; Santa Cruz Biotechnology) and CENP-F (rabbit monoclonal antibody; Novus Biologicals). The anti-TPX2 antibody was obtained from Duane A. Compton (Department of Biochemistry, Dartmouth Medical School, Hanover, NH).

Microscopy and image analyses

Cell preparations were examined using a deconvolution microscopy system (DeltaVision; Applied Precision) or by florescence microscopy (AxioPlan II; Zeiss) using oil-immersion objective lenses. The fluorescence intensities of the signals were analyzed using ImageJ software (http://rsb.info.nih.gov/ij/download.html). The inter-kinetochore distances were measured as previously described (Waters et al., 1996). The distances were determined in at least five cells (40 kinetochore pairs).

To measure the amount of target proteins associated with MTs, the intensity of the target protein channel was measured within each 0.65-μm sphere, and the mean background was subtracted. The results of these intensity measurements were

normalized by the intensity of α-tubulin. The intensities of cold-stable MTs were quantified as previously described (Toso et al., 2009). In brief, the intensity of tubulin was measured within each 0.7-μm sphere, and the mean background was subtracted. For each siRNA condition, the individual intensities of cold-stable kinetochore fibers were determined in five cells with at least 30 kinetochores per cell, yielding a distribution of at least 150 kinetochore fiber intensities. The distribution in control cells was subdivided into four categories. Values below background or values between 0 and 100 were designated kinetochores with weak attachments, values from 101 to 350 were categorized as medium attachments, and values above 350 were considered strong attachments. All of the intensities were measured using ImageJ.

For cell imaging of living cells, the medium was replaced with a CO_2-independent medium supplemented with 10% fetal bovine serum, penicillin/streptomycin and L-glutamine (Invitrogen). Cells were maintained at 37°C using a heated stage. Images of cells expressing GFP–H1.2 were recorded under an inverted microscope (Olympus IX81) using a 40× NA 1.4 PlanApo objective. MetaMorph software (Universal Imaging) was used to control the acquisition parameters, including exposure, focus and illumination. Single focal plane images were collected by a camera at 3-minute intervals. To capture images of cells expressing YFP–α-tubulin, the CSU10 confocal microscopy system (Yokogawa) was used. Images were acquired at 10-second time intervals. All subsequent analyses and processing of images were performed using MetaMorph software.

Immunostaining of HeLa cells

HeLa cells on poly-L-lysine-coated coverslips were fixed in 4% PFA in PBS for 10 minutes at 37°C and then permeabilized in 0.2% Triton X-100 in PBS for 10 minutes. To examine stabilization of kinetochore–MTs, the cells were incubated at 4°C for 10 minutes before fixation. Next, the cells were blocked with 1% BSA in PBS for 30 minutes, and sequentially incubated with the primary and secondary antibodies diluted in 1% BSA in PBS for 1 hour each. All incubations were done at 37°C. For some antibodies (CENP-E and γ-tubulin), immunostaining was performed as previously described (Forgues et al., 2003). For Bub1, TPX2, Aurora A, CENP-F and SAF-A staining, the cells were fixed in methanol for 10 minutes at –20°C.

Immunoblotting

After extraction of transfected cells with SDS sample buffer, the protein extracts were separated by SDS-PAGE and transferred to PVDF membranes for immunoblotting. Immunoblots were blocked with 0.1% BSA in TBST buffer (0.1% Tween 20, 25 mM Tris-HCl pH 7.4, 137 mM NaCl, 25 mM KCl) and then sequentially incubated with primary and secondary antibodies diluted in TBST. Finally, the immunoreactive protein bands were detected by NBT/BCIP solution (Roche) supplemented with alkaline phosphatase buffer (100 mM Tris-HCl pH 9.5, 100 mM NaCl, 1 mM $MgCl_2$).

Immunoprecipitation

Immunoprecipitation was performed using antibodies against nucleolin, Aurora-A and TPX2 (Bethyl Laboratories). Normal mouse or rabbit IgG (Santa Cruz Biotechnology) was used as a control. The antibodies were bound to protein G–Sepharose (GE Healthcare) in buffer A (0.1% BSA, 150 mM NaCl, 20 mM Tris-HCl pH 8.0 and 0.05% Tween 20), by rocking at 4°C overnight. HeLa cells were harvested by centrifugation at 200 ***g*** for 5 minutes, rinsed with PBS and centrifuged. The cell pellets were stored at –80°C. The cells were extracted in five volumes of lysis buffer [10% cell lysis buffer (Cell Signaling), 0.1% SDS, 10% glycerol, protease inhibitor cocktail (Roche)] for 30 minutes, and centrifuged at 15,000 ***g*** for 30 minutes. To reduce the amount of nonspecific protein binding, the supernatant was first rocked with the beads for 30 minutes at 4°C. After centrifugation, the supernatant was incubated with the antibody–bead complexes for 3 hours at 4°C. Next, the beads were collected by centrifugation and washed five times in lysis buffer. Finally, the protein–bead complexes were solubilized by boiling, then centrifuged, subjected to SDS-PAGE and analyzed by immunoblotting.

Flow cytometry analysis

The cells were transfected with SAF-A-specific siRNAs and incubated for 72 hours. The cells were incubated with trypsin–EDTA at 37°C for 5 minutes, after which the aspirated medium was used to reconstitute the cells. For propidium iodide (PI) staining, the cells were incubated with 0.1% sodium citrate hypotonic solution containing 0.25 mg/ml RNaseA and 50 μg/ml PI for 30 minutes at 4°C. The PI-stained cells were incubated for another 15 minutes at 37°C for RNA degradation. Finally, the cells were subjected to EPICS ALTRA cell sorting system (Beckman Coulter) as previously described (Gambe et al., 2009).

In vitro phosphorylation assay

The in vitro phosphorylation assay was performed using purified GST-H3(5-15) and isolated SAF-A from 60 l of HeLa suspension culture (Vaxron, Rockaway, NJ) as substrates and a recombinant Aurora-A from *Escherichia coli* as the kinase, as previously described (Ohashi et al., 2006).

Microtubule binding assay

Microtubules (final concentration: 4 μM) were assembled from purified tubulins (Cytoskeleton) in general tubulin buffer (80 mM PIPES, 2 mM $MgCl_2$, 1 mM EGTA, pH 7.0) containing 1 mM GTP and 10% glycerol at 35°C for 20 minutes. The microtubules were immediately stabilized with 20 μM taxol and incubated for another 20 minutes. Isolated SAF-A and recombinant TPX2 (OriGene Technologies) were added to the taxol-stabilized microtubules, and incubated at 30°C for 30 minutes. The reaction mixture was pelleted through a 40% glycerol cushion containing 20 μM taxol in general tubulin buffer at 20,000 ***g*** for 120 minutes at 25°C.

This work was supported by Grants-in-Aid for Scientific Research from the Ministry of Education, Science, Culture, Sports, Science and Technology of Japan to K.F. and S.M., and by grants from the Japan Science and Technology Agency (SENTAN to K.F. and BIRD to S.M.). A.M. was supported by a Research Fellowship from the Japanese Society for the Promotion of Science for Young Scientists. We thank Duane A. Compton for the anti-TPX2 antibody, Masanori Noda for protein identification and Shuichi Aikawa for flow cytometry.

Supplementary material available online at
http://jcs.biologists.org/cgi/content/full/124/3/394/DC1

References

Barr, A. R. and Gergely, F. (2007). Aurora-A: the maker and breaker of spindle poles. *J. Cell Sci*. **120**, 2987-2996.

Bayliss, R., Sardon, T., Vernos, I. and Conti, E. (2003). Structural basis of Aurora-A activation by TPX2 at the mitotic spindle. *Mol. Cell* **12**, 851-862.

Berglund, F. M. and Clarke P. R. (2009). hnRNP-U is a specific DNA-dependent protein kinase substrate phosphorylated in response to DNA double-strand breaks. *Biochem. Biophys. Res. Commun*. **381**, 59-64.

Biggins, S. and Walczak, C. E. (2003). Captivating capture: How microtubules attach to kinetochores. *Curr. Biol.* **13**, 449-460.

Bird, A. W. and Hyman, A. A. (2008). Building a spindle of the correct length in human cells requires the interaction between TPX2 and Aurora A. *J. Cell Biol.* **182**, 289-300.

Blagden, S. P. and Glover, D. M. (2003). Polar expeditions-provisioning the centrosome for mitosis. *Nat. Cell Biol.* **5**, 505-511.

Compton, D. A., Szilak, I. and Cleveland, D. W. (1992). Primary structure of NuMA, an intranuclear protein that defines a novel pathway for segregation of proteins at mitosis. *J. Cell Biol.* **116**, 1395-1408.

Dreyfuss, G., Choi, Y. D. and Adam, S. A. (1984). Characterization of heterogeneous nuclear RNA-protein complexes in vivo with monoclonal antibodies. *Mol. Cell. Biol.* **4**, 1104-1114.

Fackelmayer, F. O. and Richter, A. (1994). hnRNP-U/SAF-A is encoded by two differentially polyadenylated mRNAs in human cells. *Biochim. Biophys. Acta.* **1217**, 232-234.

Forgues, M., Difilippantonio, M. J., Linke, S. P., Ried, T., Nagashima, K., Feden, J., Valerie, K., Fukasawa, K. and Wang, X. W. (2003). Involvement of Crm1 in hepatitis B virus X protein-induced aberrant centriole replication and abnormal mitotic spindles. *Mol. Cell. Biol.* **23**, 5282-5292.

Gambe, A. E., Matsunaga, S., Takata, H., Ono-Maniwa, R., Baba, A., Uchiyama, S. and Fukui, K. (2009). A nucleolar protein RRS1 contributes to chromosome congression. *FEBS Lett.* **583**, 1951-1956.

Gambe, A. G., Ono-Maniwa, R., Matsunaga, S., Kutsuna, N., Higaki, T., Higashi, T., Hasezawa, S., Uchiyama, S. and Fukui, K. (2007). Development of a multistage classifier for a monitoring system of cell activity based on imaging of chromosomal dynamics. *Cytometry A* **71**, 286-296.

Garrett, S., Auer, K., Compton, D. A. and Kapoor, T. M. (2002). hTPX2 is required for normal spindle morphology and centrosome integrity during vertebrate cell division. *Curr. Biol.* **12**, 2055-2059.

Girdler, F., Gascoigne, K. E., Eyers, P. A., Hartmuth, S., Crafter, C., Foote, K. M., Keen, N. J. and Taylor, S. S. (2006). Validating Aurora B as an anti-cancer drug target. *J. Cell Sci.* **119**, 3664-3675.

Glover, D. M. (2003). Aurora A on the mitotic spindle is activated by the way it holds its partner. *Mol. Cell* **12**, 797-799.

Gohring, F., Schwab, B. L., Nicotera, P., Leist, M. and Fackelmayer, F. O. (1997). The novel SAR-binding domain of scaffold attachment factor A (SAF-A) is a target in apoptotic nuclear breakdown. *EMBO J.* **16**, 7361-7371.

Gruss, O. J., Carazo-Salas, R. E., Schatz, C. A., Guarguaglini, G., Kast, J., Wilm, M., Le Bot, N., Vernos, I., Karsenti, E. and Mattaj, I. W. (2001). Ran induces spindle assembly by reversing the inhibitory effect of importin alpha on TPX2 activity. *Cell* **104**, 83-93.

Gruss, O. J., Wittmann, M., Yokoyama, H., Pepperkok, R., Kufer, T., Sillje, H., Karsenti, E., Mattaj, I. W. and Vernos, I. (2002). Chromosome-induced microtubule assembly mediated by TPX2 is required for spindle formation in HeLa cells. *Nat. Cell Biol.* **4**, 871-879.

Hirota, T., Kunitoku, N., Sasayama, T., Marumoto, T., Zhang, D., Nitta, M., Hatakeyama, K. and Saya, H. (2003). Aurora-A and an interacting activator, the LIM protein Ajuba, are required for mitotic commitment in human cells. *Cell* **114**, 585-598.

Hutchins, J. R., Toyoda, Y., Hegemann, B., Poser, I., Heriche, J. K., Sykora, M. M., Augsburg, M., Hudecz, O., Buschhorn, B. A., Bulkescher, J. et al. (2010). Systematic analysis of human protein complexes identifies chromosome segregation proteins. *Science* **328**, 593-599.

Jost, E., Lepper, K., Hogner, D., Zimmer, A. and Boschek, B. (1986). Redistribution of nuclear lamins in mitotic cells. *Biol. Cell* **57**, 111-126.

Katayama, H., Sasai, K., Kloc, M., Brinkley, B. R. and Sen, S. (2008). Aurora kinase-A regulates kinetochore/chromatin associated microtubule assembly in human cells. *Cell Cycle* **7**, 2691-2704.

Kirschner, M. and Mitchison, T. (1986). Beyond self-assembly: from microtubules to morphogenesis. *Cell* **45**, 329-342.

Kufer, T. A., Sillje, H. H. W., Korner, R., Gruss, O. J., Meraldi, P. and Nigg, E. A. (2002). Human TPX2 is required for targeting Aurora-A kinase to the spindle. *J. Cell Biol.* **158**, 617-623.

Kufer, T. A., Nigg, E. A. and Sillje, H. H. (2003). Regulation of Aurora-A kinase on the mitotic spindle. *Chromosoma* **112**, 159-163.

Kukalev, A., Nord, Y., Palmberg, C., Bergman, T. and Percipalle, P. (2005). Actin and hnRNP U cooperate for productive transcription by RNA polymerase II. *Nat. Struct. Mol. Biol.* **12**, 238-244.

Kunitoku, N., Sasayama, T., Marumoto, T., Zhang, D., Honda, S., Kobayashi, O., Hatakeyama, K., Ushio, Y., Saya, H. and Hirota, T. (2003). CENP-A phosphorylation by Aurora-A in prophase is required for enrichment of Aurora-B at inner centromeres and for kinetochore function. *Dev. Cell* **5**, 853-864.

Li, N., Yuan, K., Yan, F., Huo, Y., Zhu, T., Liu, X., Guo, Z. and Yao, X. (2009). PinX1 is recruited to the mitotic chromosome periphery by Nucleolin and facilitates chromosome congression. *Biochem. Biophys. Res. Commun.* **384**, 76-81.

Ma, N., Matsunaga, S., Takata, H., Ono-Maniwa, R., Uchiyama, S. and Fukui, K. (2007). Nucleolin functions in nucleolus formation and chromosome congression. *J. Cell Sci.* **120**, 2091-2105.

Manning, A. L. and Compton, D. A. (2007). Mechanisms of spindle-pole organization are influenced by kinetochore activity in mammalian cells. *Curr. Biol.* **17**, 260-265.

Marumoto, T., Honda, S., Hara, T., Nitta, M., Hirota, T., Kohmura, E. and Saya, H. (2003). Aurora-A kinase maintains the fidelity of early and late mitotic events in HeLa cells. *J. Biol. Chem.* **278**, 51786-51795.

Nickerson, J. A., Krockmalnic, G., Wan, K. M., Turner, C. D. and Penman, S. (1992). A normally masked nuclear matrix antigen that appears at mitosis on cytoskeleton filaments adjoining chromosomes, centrioles, and midbodies. *J. Cell Biol.* **116**, 977-987.

Nousiainen, M., Sillje, H. H., Sauer, G., Nigg, E. A. and Korner, R. (2006). Phosphoproteome analysis of the human mitotic spindle. *Proc. Natl. Acad. Sci. USA* **103**, 5391-5396.

Ohashi, S., Sakashita, G., Ban, R., Nagasawa, M., Matsuzaki, H., Murata, Y., Taniguchi, H., Shima, H., Furukawa, K. and Urano, T. (2006). Phospho-regulation of human protein kinase Aurora-A: analysis using anti-phospho-Thr288 monoclonal antibodies. *Oncogene* **25**, 7691-7702.

Podgornaya, O. I., Voronin, A. P., Enukashvily, N. I., Matveev, I. V. and Lobov, I. B. (2003). Structure-specific DNA-binding proteins as the foundation for three-dimensional chromatin organization. *Int. Rev. Cytol.* **224**, 227-296.

Rieder, C. L. (1981). The structure of the cold-stable kinetochore fiber in metaphase PtK1 cells. *Chromosoma* **84**, 145-158.

Roming, H., Fackelmayer, F. O., Renz, A., Ramsperger, U. and Richter, A. (1992). Characterization of SAF-A, a novel nuclear DNA binding protein from HeLa cells with high affinity for nuclear matrix/scaffold attachment DNA elements. *EMBO J.* **11**, 3431-3440.

Sardon, T., Peset, I., Petrova, B. and Vernos, I. (2008). Dissecting the role of Aurora A during spindle assembly. *EMBO J.* **27**, 2567-2579.

Sauer, G., Korner, R., Hanisch, A., Ries, A., Nigg, E. A. and Sillje, H. H. (2005). Proteome analysis of the human mitotic spindle. *Mol. Cell. Proteomics* **4**, 35-43.

Spraggon, L., Dudnakova, T., Slight, J., Lustig-Yariv, O., Cotterell, J., Hastie, N. and Miles, C. (2007). hnRNP-U directly interacts with WT1 and modulates WT1 transcriptional activation. *Oncogen* **26**, 1484-1491.

Stenoien, D. L., Sen, S., Mancini, M. A. and Brinkley, B. R. (2003). Dynamic association of a tumor amplified kinase, Aurora-A, with the centrosome and mitotic spindle. *Cell Motil. Cytoskeleton* **55**, 134-146.

Tanenbaum, M. E., Macurek, L., Janssen, A., Geers, E. F., Alvarez-Fernandez, M. and Medema, R. H. (2009). Kif15 cooperates with eg5 to promote bipolar spindle assembly. *Curr. Biol.* **19**, 1703-1711.

Tang, Z., Sun, Y., Harley, S. E., Zou, H. and Yu, H. (2004). Human Bub1 protects centromeric sister-chromatid cohesion through Shugoshin during mitosis. *Proc. Natl. Acad. Sci. USA* **101**, 18012-18017.

Toso, A., Winter, J. R., Garrod, A. J., Amaro, A. C., Meraldi, P. and McAinsh, A. D. (2009). Kinetochore-generated pushing forces separate centrosomes during bipolar spindle assembly. *J. Cell Biol.* **184**, 365-372.

Tulu, U. S., Fagerstrom, C., Ferenz, N. P. and Wadsworth, P. (2006). Molecular requirements for kinetochore-associated microtubule formation in mammalian cells. *Curr. Biol.* **16**, 536-541.

Waters, B. A., Skibbens, R. V. and Salmon, E. D. (1996). Oscillating mitotic newt lung cell kinetochores are, on average, under tension and rarely push. *J. Cell Sci.* **109**, 2823-2831.

Wittmann, T., Wilm, M., Karsenti, E. and Vernos, I. (2000). TPX2, a novel *Xenopus* MAP involved in spindle pole organization. *J. Cell Biol.* **149**, 1405-1418.

Wollman, R. E., Cytrynbaum, N., Jones, J. T., Meyer, T., Scholey, J. M. and Mogilner, A. (2005). Efficient chromosome capture requires a bias in the 'search- and-capture' process during mitotic-spindle assembly. *Curr. Biol.* **15**, 828-832.

Yanagida, M., Shimamoto, A., Nishikawa, K., Furuichi, Y., Isobe, T. and Takahashi, N. (2001). Isolation and proteomic characterization of the major proteins of the nucleolin-binding ribonucleoprotein complexes. *Proteomics* **1**, 1390-1404.

Yuan, K., Li, N., Jiang, K., Zhu, T., Huo, Y., Wang, C., Lu, J., Shaw, A., Thomas, K., Zhang, J. et al. (2009). PinX1 is a novel microtubule-binding protein essential for accurate chromosome segregation. *J. Biol. Chem.* **284**, 23072-23082.